The AMIGA infill detector of the Pierre Auger Observatory: performance and first data

IOANA C. MARIŞ[1] FOR THE PIERRE AUGER COLLABORATION[2]

[1]*Laboratoire de Physique Nucléaire et des Hautes Energies, Universités Paris 6 et Paris 7, CNRS-IN2P3, Paris, France*
[2]*Observatorio Pierre Auger, Av. San Martín Norte 304, 5613 Malargüe, Argentina*
(Full author list: http://www.auger.org/archive/authors_2011_05.html)
auger_spokepersons@fnal.gov

Abstract: We present a first analysis of cosmic rays observed with the AMIGA infill array of the Pierre Auger Observatory. The spacing of 750 m between the surface detectors, half the distance of the regular array, allows us to extend the energy range of interest to energies as low as 3×10^{17} eV. The lateral distribution function is presented and the uncertainty of the signal at an optimum distance of 450 m, used to obtain an energy estimator, is discussed. The first steps towards the measurement of the energy spectrum are described. The calculation of the array exposure and the strategy for the energy calibration of the infill, obtained from events observed in coincidence with the fluorescence detector, are presented.

Keywords: Pierre Auger Observatory, very high energy cosmic rays, AMIGA infill array

1 Introduction

The energy range between 10^{17} eV and 4×10^{18} eV is of great interest for understanding the origin of cosmic rays. At these energies the transition from the galactic to extragalactic accelerators [1, 2, 3] is expected. Also a spectral feature caused by the drop of the heavy component of the galactic cosmic rays [4] has been predicted. The Pierre Auger Observatory [5], being the largest cosmic ray experiment in operation, has delivered important results for solving the nature of cosmic rays above an energy of 10^{18} eV. To extend the measurements to lower energies two enhancements are being built: HEAT [6] (High Elevation Auger Telescopes) and AMIGA (Auger Muons and Infill for the Ground Array) [7]. We present the performance and current status of the analysis of the data taken with the infill array of AMIGA. Construction of the infill array began in 2008: currently 53 stations (87% of the total 61) have been deployed. The detectors are on a triangular grid with a spacing of 750 m. The reconstruction procedures are adaptations of those used for the 3000 km² array where the spacing between the detectors is 1500 m. In the first part we describe the trigger efficiency and the accumulated exposure, followed by the description of the reconstruction of air-showers.

2 Trigger efficiency and acceptance

The trigger system of the infill array is adopted from the regular Auger array. An event is accepted when at least 3 stations forming a triangle satisfy a local trigger of the
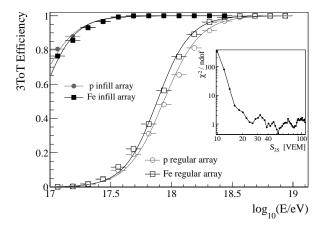

Figure 1: 3ToT trigger efficiency for the infill and regular array obtained from simulations of Iron and proton primaries. In the inset figure the reduced χ^2 for a flat dependency on the zenith angle of the trigger is depicted.

type Time-over-Threshold (3ToT event) [8]. The smaller spacing between stations of the infill lead to an increase of the trigger efficiency at low energy. The trigger efficiency as a function of energy for 3ToT events with zenith angles below 55° is illustrated in Fig. 1, for both infill and regular array. The calculation is based on the parametrization of the single station lateral trigger probability [9], which reflects the properties of the station response and of the air-shower development. A simple test of the threshold energy where the array is fully efficient is performed via a χ^2 test
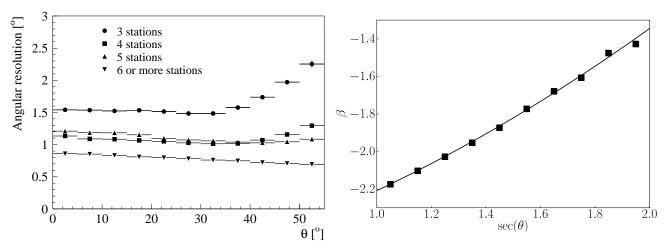
Figure 2: (left) Angular resolution for different multiplicities as a function of the zenith angle. (right) The weighted mean of the LDF parameter, β, as a function of the zenith angle. The line represents the parametrization of β.

of an isotropic flux of the observed cosmic rays. Below this energy the trigger depends on the zenith angle. The reduced χ^2 as a function of the energy estimator, S_{35}, is illustrated in the inset of Fig. 1. The trigger is independent of the zenith angle for S_{35} larger than $20\,\text{VEM}$, corresponding to an energy of $\approx 3 \times 10^{17}\,\text{eV}$. From both methods we conclude that above this energy the infill array is 100% efficient for cosmic rays with a zenith angle of less than $55°$.

To guarantee the selection of good quality and well-contained events, a fiducial cut (T5) is applied so that only events in which the station with the highest signal is surrounded by 6 working neighbors (i.e. a working hexagon) are accepted. This condition assures a good reconstruction of the impact point on ground, meanwhile allowing for a simple geometrical calculation of the aperture. The 3ToT trigger rate is (55 ± 6) events/day/hexagon out of which (28 ± 3) events/day/hexagon are T5. Integrating the instantaneous effective area over the time when the detector was stable, the acceptance between August 2008 (when the first 3 hexagons of the infill were completed) and March 2011 (16 hexagons) amounts to $(26.4 \pm 1.3)\,\text{km}^2\,\text{sr yr}$. With the current configuration we record (390 ± 70) T5 events/day and the data sample contains more than 260,000 T5 events.

3   Reconstruction of the air-showers

The reconstruction algorithm for the events triggering the infill array is based on the well-tuned code for the regular surface detector array. After selecting the signals which are generated by air-showers, the direction and the energy of the primary cosmic ray are deduced from the timing information and from the total recorded signal in the stations. The atmospheric muons can generate background signal in a time window close to the arrival of air-shower particles. The stations are selected according to their time compati-

bility with the estimated shower front. The time cuts were determined such that 99% of the stations containing a physical signal from the shower are kept. The algorithm for the signal search in the time traces rejects further accidental signals by searching for time-compatible peaks.

Angular resolution: The arrival direction is obtained from the time propagation of the shower front on the ground which is approximated as a sphere with the origin on the shower axis traveling with the speed of light. To obtain the angular resolution [10] the single station time variance is modeled to take into account the size of the total signal and its time evolution. The angular resolution achieved, illustrated in Fig. 2(left), for events with more than 3 stations is better than $1.3°$ and is better than $1°$ for events with more than 6 stations.

Lateral distribution function: The impact point on ground of the air showers is deduced in the fit of the lateral distribution of the signals as well. The fit of the lateral distribution function (LDF) [11] is based on a maximum likelihood method which also takes into account the probabilities for the stations that did not trigger and the stations close to the shower axis which are saturated. The saturation is caused by the overflow of the FADC read-out electronics and a modification of the signal occurs due to the transition of the PMTs from a linear to a non-linear behavior. Two functions have been investigated to describe the lateral distribution of the signals on ground: a log-log parabola (LLP), used in the current analysis to infer the systematic uncertainties due to the LDF assumption, and a modified Nishimura-Kamata-Greisen (NKG) function:

$$S(r) = S(r_\text{opt}) \left(\frac{r}{r_\text{opt}} \frac{r + 700\,\text{m}}{r_\text{opt} + 700\,\text{m}} \right)^\beta \qquad (1)$$

where r_opt is the optimum distance and $S(r_\text{opt})$ is used to obtain an energy estimator. The parameter β depends on zenith angle and on energy. For events with only 3 stations
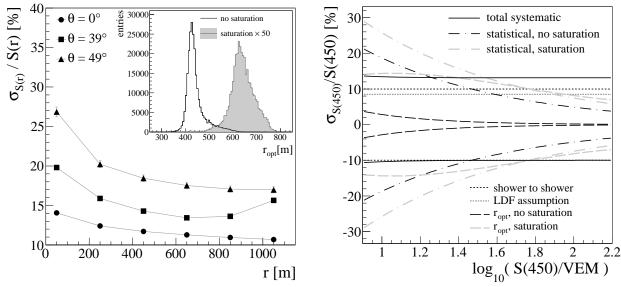
Figure 3: (left) The relative uncertainty of the signal as a function of the distance to the shower axis for different zenith angles deduced from simulations of a mixed composition (50% p, 50% Fe) at 5.62×10^{17} eV. The distributions of the optimum distance obtained from data for the events without saturation and for events with a saturated signal (multiplied by 50, gray) are shown in the inset. (right) Relative statistical and systematic uncertainties of S(450). For the description of different contributions see text.

the reconstruction of the air-showers can be obtained only by fixing the β parameter. To obtain the parametrization of β, shown in Fig. 2(right), events with more than 6 stations are selected. The vertical events are observed at an earlier shower age than the inclined ones, thus having a steeper LDF due to the different contributions from the muonic and electromagnetic components on ground. The dependence of the LDF parameters on the energy is under investigation.

Optimum distance and uncertainties of S(450): The optimum distance is defined as the distance from the shower axis where the fluctuations of the LDF are minimized and it is mostly determined by the spacing between the detectors [12]. In Fig. 3(left) the relative uncertainties of the signals at different distances from the shower axis are illustrated for simulations of a mixed composition (50% proton and 50% iron) at an energy of 5.62×10^{17} eV and different zenith angles. The air-shower simulations were performed with CORSIKA [13], using QGSJet-II [14] and Fluka [15], and the detector simulation were based on Offline [16]. The uncertainties, containing the shower-to-shower fluctuations, are minimized at distances larger than 450 m.

From data we obtained the distance where the LDF is least sensitive to the β parameter by performing the reconstruction of the same event with different β values within the uncertainties of the parametrization. This is illustrated in the inset of Fig. 3(left). Similar to the regular array [17], we distinguish the events where the signal in the station closest to the shower axis is saturated. The mean of the distribution of the distance to the shower axis where the impact of the LDF is minimal, for the events without saturated signals is (442.3 ± 0.1) m with a RMS of (40.33 ± 0.06) m,

while for the events with at least a saturated signal is (639.1 ± 0.1) m with a RMS of (51.64 ± 0.06) m. The signal at $r_{\mathrm{opt}} = 450$ m, S(450), was chosen to obtain an energy estimator.

The statistical and systematic uncertainties of S(450) as a function of $\log_{10} S(450)$ are illustrated in Fig. 3(right). The parametrizations were obtained from data similar to the regular array [17]. The statistical uncertainties of S(450) vary from 20 % at 10 VEM to 5 % at 100 VEM. The events in which at least one signal is saturated have an uncertainty that is larger by $\approx 10\%$. The r_{opt} changes from event to event. The contribution of the variations of r_{opt} to the uncertainty of S(450) was obtained by reconstructing the same event with different β values. While this effect is negligible for the accuracy of S(450) for events without saturation, it contributes with 15% to the total uncertainty for saturated events. The relative difference of the S(450) obtained using a LLP to the estimation from a NKG function is +8.5%. This systematic uncertainty cancels in the final energy resolution via the cross-calibration with the fluorescence detector energy. Preliminary estimations let us assume that the shower-to-shower fluctuations contribute with 10% to the total uncertainty.

Attenuation in the atmosphere: S(450) is corrected for the zenith angle dependency caused by the shower attenuation in the atmosphere with a constant intensity cut method [18]. The zenith angle correction has been deduced empirically to be a second degree polynomial in $x = \cos^2 \theta - \cos^2 35°$. The zenith angle of 35° represents the median of the distribution of the arrival directions of the observed cosmic rays. The equivalent signal at 35°, S_{35} is used to infer the energy: $S_{35} = S(450)/(1+(1.59\pm$
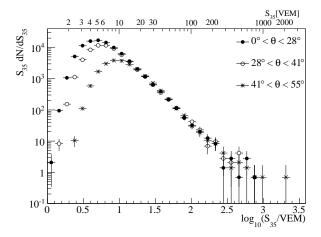
Figure 4: The distribution of events as a function of $\log_{10}(S_{35}/\text{VEM})$ for different zenith angle intervals.
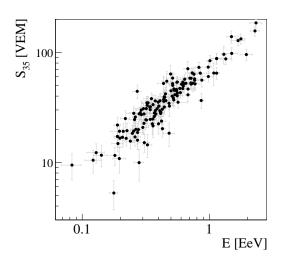

Figure 5: The correlation between S_{35} and energy.

$0.05)x - (1.14 \pm 0.21)x^2)$. The number of events as a function of S_{35} is illustrated in Fig. 4 for different zenith angle intervals. The trigger threshold effect can be seen below 20 VEM. The S_{35} spectrum extends to more than 2000 VEM, corresponding to an energy of $\approx 3 \times 10^{19}\,\text{eV}$.

Energy calibration: The energy calibration of the surface detector data is obtained from air-showers that were simultaneously measured with the fluorescence detector (i.e. hybrid events). At energies lower than $10^{18}\,\text{eV}$ due to its field of view, the fluorescence detector observes more deep showers than shallow ones. Therefore it is necessary to apply a fiducial field of view cut [19] that ensures an unbiased energy calibration. The selection criteria and the energy systematic uncertainties are currently under study. S_{35} shows a strong correlation with the energy as it is illustrated in Fig. 5 for the selected [18] hybrid events.

4 Conclusions

The infill detector, part of the AMIGA experiment, has been operating in good conditions since its deployment. It extends the energy range for the surface detector of Pierre Auger Observatory down to $3 \times 10^{17}\,\text{eV}$. The analysis, based on the algorithms developed for the regular array is in an advanced stage. The integrated exposure between August 2008 and March 2011 is $(26.4 \pm 1.3)\,\text{km}^2\,\text{sr yr}$. The achieved angular resolution is better than 1 degree for an energy of $3 \times 10^{17}\,\text{eV}$. The resolution of S(450) varies from 20% at 10 VEM to 10% at 100 VEM, at the highest energies being dominated by shower-to-shower fluctuations. The studies on the selection of hybrid events used for the energy calibration and on the energy systematic uncertainties are in progress.

References

[1] V. Berezinsky, A. Z. Gazizov, and S. I. Grigorieva, Phys. Lett., 2005, **B612**:147

[2] A.M. Hillas, J. Phys., 2005, **G31**:R95

[3] T. Wibig and A.W. Wolfendale., J. Phys., 2005, **G31**:255

[4] J.R. Hörandel, Astropart. Phys.,2003, **19(2)**:193

[5] The Pierre Auger Collaboration, Nucl. Instrum. Meth. in Phys., 2004, **A 523**:50

[6] H.J. Mathes for the Pierre Auger Collaboration, paper 0761, these proceedings

[7] F. Sanchez for the Pierre Auger Collaboration, paper 0742, these proceedings

[8] The Pierre Auger Collaboration, Nucl. Instrum. Meth. in Phys., 2010, **A 613**:29

[9] The Pierre Auger Collaboration, The Lateral Trigger Probability function for UHE Cosmic Rays Showers detected by the Pierre Auger Observatory, submitted to Astropart. Phys., 2011

[10] C. Bonifazi for the Pierre Auger Collaboration, Nucl. Phys. B Proc. Suppl., 2009, **190**:20

[11] D. Barnhill for the Pierre Auger Collaboration, Proc. 29th ICRC, Pune, India, 2005, **7**:291

[12] D. Newton, J. Knapp, A.A. Watson, Astroparticle Physics, 2007, **26**:414

[13] D. Heck et al., 1998, FZKA-6019

[14] S. Ostapchenko, Phys. Rev., 2006, **D74**: 014026; N.N. Kalmykov et al. Nucl. Phys. (Proc. Suppl.), 1997, **B52**:17

[15] G. Battistoni et al., AIP Conf. Proc., 2007, **896**:31

[16] S. Argiro et al., Nucl. Instrum. Meth., 2007, **A580**:1485

[17] M. Ave for the Pierre Auger Collaboration, Proc. 30th ICRC, Merida, Mexico, 2008, **4**:307

[18] R. Pesce for the Pierre Auger Collaboration, paper 1160, these proceedings

[19] The Pierre Auger Collaboration, Phys. Rev. Lett., 2010, **104**:091101